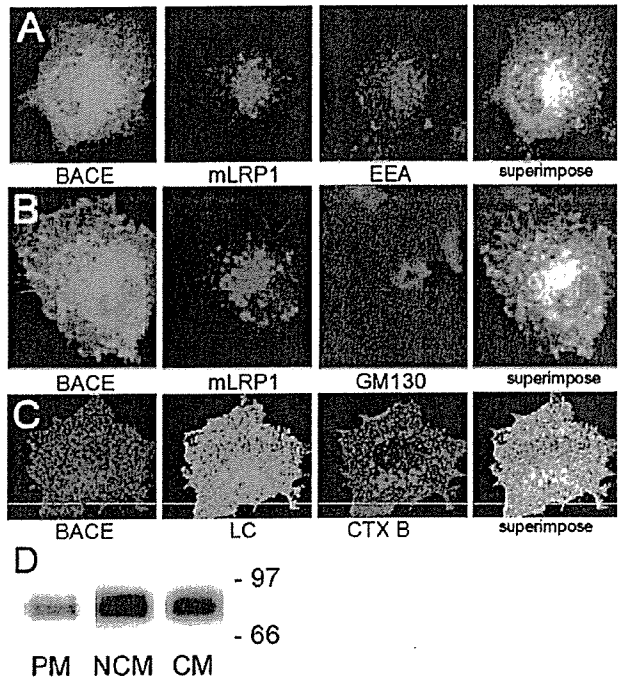

FIG. 2. **Localization of BACE and mLRP1 in transfected cells.** *A*, BACE-V5 (*green*) and mLRP1-Myc (*red*) co-transfected H4 cells were immunostained with anti-V5 mAb (visualized by Cy5) and rabbit anti-Myc Ab (visualized by Cy3) followed by a FITC-conjugated antibody to the endosomal marker EEA1 (shown in *blue*). *B*, BACE-GFP (*green*) and mLRP1-Myc (*red*) were co-transfected and then immunostained with rabbit anti-Myc (visualized by Cy3) and an antibody to the Golgi marker GM130 (visualized by Cy5, shown in *blue*). *C*, to demonstrate cell surface localization, BACE-V5 (*blue*) and Myc-(N terminus)-LC (*green*) were co-transfected and then immunostained with anti-Myc mAb (visualized by FITC) and rabbit anti-BACE-NT Ab (visualized by Cy5) without permeabilizing the cell membrane. Alexa-555-labeled cholera toxin B (*CTx-B*), used to visualize lipid rafts, was added for 20 min after thoroughly washing the primary and before adding the secondary Ab. *D*, total plasma membrane (*PM*) fraction along with CM and NCM membrane fractions immunoprecipitated with anti-LRP monoclonal 5A6 were separated on 4–12% SDS-PAGE and analyzed by immunoblot analysis using ^{125}I-anti-LRP monoclonal 11H4.

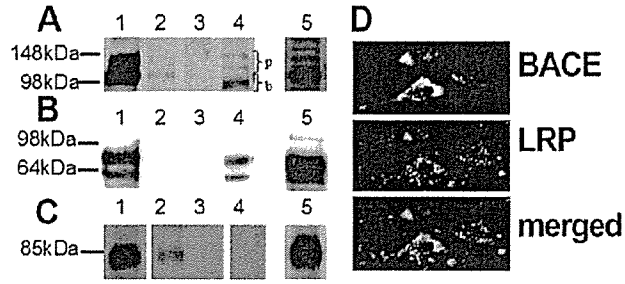

FIG. 3. **LRP and BACE in human brain.** *A*, extracts from mLRP1-Myc and BACE-V5-transfected H4 cells were immunoprecipitated with mouse anti-V5 Ab and probed with rabbit anti-Myc Ab. Anti-Myc recognizes precursor endoplasmic reticulum and Golgi forms (labeled *p*) as well as β-chains of mature proteins (labeled *b*) (positive control, *lane 5*) (29). Specific bands of all isoforms were found in pull-downs (*lane 1*) from lysates of mLRP1-Myc- and BACE-V5-expressing cells. *B*, immunoprecipitates of mLRP1-Myc were probed with an anti-BACE Ab, showing immunoreactive bands for BACE (~60 and 75kDa) in *lane 1*. The 60-kDa band represents endogenous BACE and the 75-kDa band transfected BACE-V5 (*lane 5*). *C*, human brain extracts were immunoprecipitated with rabbit anti-BACE-CT Ab and probed with 11H4. LC is recognized as an 85-kDa band brain homogenate (*lane 5*). A specific band of the same size was found after co-immunoprecipitation with anti-BACE-Ab (*lane 1*). Identical results were observed when probing with 5A6, another LC-specific Ab (data not shown). Negative controls as described above are shown in *lanes 2* and *3*. Supernatants are shown in *lane 4*. *D*, BACE and LRP co-localization in human brain tissue is shown by confocal microscopy.

blocked in 5% nonfat dried milk. mLRP1-Myc was detected by rabbit anti-Myc Ab. BACE was detected by rabbit anti-BACE-NT Ab. Secondary antibodies conjugated to horseradish peroxidase were applied and visualized by chemiluminescence. The Massachusetts Alzheimer Disease Research Center Brain Bank provided temporal cortex. Our protein solubilization procedure was adapted from previously reported studies (35) with minor modifications. The tissue was homogenized at 1 ml/100 mg tissue in ice-cold TEVP-sucrose buffer (containing 10 mM Tris, pH 7.4, 5 mM NaF, 1 mM Na_3VO_4, 1 mM EDTA, 1 mM EGTA, and 320 mM sucrose). The homogenates were centrifuged at 4 °C, and the supernatants were removed. The pellets were resuspended in 800 μl of TEVP with 1% SDS, sonicated for 10 s, and then boiled for 5 min. The samples were centrifuged, and the supernatant was collected for immunoprecipitation after the protein concentration was determined by protein assay (Bio-Rad). Co-immunoprecipitation in human brain tissue was performed as described above with rabbit anti-BACE-CT as pull-down Ab and probed with 11H4 mAb.

FRET Measurements using Fluorescence Lifetime Imaging Microscopy (FLIM)—FRET is observed when two fluorophores are in very close proximity, *i.e.* <0 nm. FRET measurements using FLIM relies on the observation that fluorescence lifetimes (the time of fluorophore emission after brief excitation, measured in picoseconds) are shorter in the presence of a FRET acceptor. We have utilized a new FLIM technique that can detect protein-protein proximity using multiphoton microscopy (36, 37). A mode-locked Ti-sapphire laser (Spectra Physics) sends a ~100-fs pulse every ~12.5 ns to excite the fluorophore. Images were acquired using a Bio-Rad Radiance 2000 multiphoton microscope. We used a high speed Hamamatsu MCP detector (MCP5900; Hamamatsu, Ichinocho, Japan) and hardware/software from Becker and Hickl (SPC 830, Berlin, Germany) to measure fluorescence lifetimes on a pixel-by-pixel basis. Excitation at 800 nm was empirically determined to excite GFP, Alexa 488 and FITC, but not Cy3. Donor fluorophore (GFP, Alexa 488, or FITC) lifetimes were fit to two exponential decay curves to calculate the fraction of fluorophores within each pixel that interact with an acceptor. As a negative control, GFP, Alexa 488, or FITC lifetimes were measured in the absence of acceptor (Cy3), which showed lifetimes equivalent to GFP, Alexa 488-IgG, or FITC IgG alone, in solution or with co-transfection with an empty vector (pEGFP) measured in the presence of Cy3-labeled BACE-V5 or LC-Myc. No bleedthrough or mis-excitation of Cy3 was observed under these conditions. Statistical testing was performed by Student's *t* test.

Internalization Assay—To quantitate BACE internalization we modified a previously reported protocol (38). CHO 13-5-1 (LRP-null cells) were grown to 70% confluency in 6-well plates and transiently transfected with Myc-BACE and either empty vector or LC-GFP. Cells were then washed once with ice-cold PBS containing 1 mM $CaCl_2$ and 1 mM $MgCl_2$, 0.2% bovine serum albumin, and 5 mM glucose (PBS++++) and 0.4 μg/ml biotinylated Myc-mAb (Upstate Biotechnologies) in PBS++++ was applied for 30 min on ice. After that the cells were allowed to endocytose at 37 °C for the indicated times. Returning the plates to ice stopped endocytosis. Surface biotin was masked with streptavidin (Roche Applied Science) for 1 h on ice. Avidin was quenched with 0.5 mg/ml biocytin (Sigma). Cells were harvested in blocking buffer (1% Triton X-100, 0.1% SDS, 0.2% bovine serum albumin, 50 mM NaCl, 1 mM Tris, pH 7.4) and incubated on IgG-coated 96-well plates at 4 °C overnight. After three washes in PBS, the plates were incubated in streptavidin-peroxidase 1:5000 (Roche Applied Science) in blocking buffer for 1 h. After another wash cycle 3× in PBS, the plates were incubated with 200 μl of 10 mg of *o*-phenyldiamine HCl (Sigma), 10 μl of 30% H_2O_2 (Sigma) in 25 ml of 50 mM Na_2HPO_4, 27 mM citrate, pH 5.0. The reaction was terminated by the addition of 50 μl of H_2SO_4 and the A_{490} was read. BACE internalization was then graphed as the percentage of internalized Myc-BACE of total surface Myc-BACE.

LRP Ectodomain Secretion Assay—HEK cells passaged into 12-well plates were transfected with a β-galactosidase reporter, LRPβ-fused N-terminally to secreted alkaline phosphatase and either empty vector, BACE, or a catalytically inactive BACE mutant. Each condition was transfected in triplicate except for siRNA experiments, which were transfected in duplicate. Media was changed 24 h later, and then collected after another 24 h. Measurement of SEAP activity in the conditioned media was carried out in triplicate by chemiluminescent assay (Roche Applied Science) according to the manufacturer's instructions. SEAP activity was normalized to β- galactosidase activity, which

TABLE I

FLIM assay data for proximity of various LRP and BACE-constructs in transfected H4 cells

If there is no interaction, lifetimes of the donor fluorophore are similar to the negative control (lacking the acceptor fluorophore). Statistically shorter lifetimes between BACE and mLRP1 regardless of the combination of fluorophore at their C terminus indicate FRET between them. To further determine the interaction site of BACE and LRP, FLIM between deletion constructs was performed.

Donor	Acceptor	Lifetime	*n*	Significance (compared to control)
		ps mean ± S.D.		
BACE-V5 (FITC)	None	2334 ± 72	12	—[a]
BACE-V5 (FITC)	mLRP1-Myc (Cy3)	2153 ± 55	11	$p < 0.0001$
mLRP1-Myc (FITC)	None	2260 ± 109	17	—[a]
mLRP1-Myc (FITC)	BACE-V5 (Cy3)	1703 ± 401	15	$p < 0.0001$
mLRP1-GFP	None	2164 ± 10	5	—
mLRP1-GFP	BACE-V5 (Cy3)	1165 ± 8	5	$p < 0.0001$
mLRP1-GFP	Myc-BACE (Cy3)	2247 ± 102	5	NS[b]
BACE-GFP	None	2284 ± 20	6	—
BACE-GFP	mLRP1-Myc (Cy3)	1756 ± 50	4	$p = 0.0004$
pEGFP-N1-vector	None	2157 ± 71	5	—
pEGFP-N1-vector	BACE-V5 (Cy3)	2106 ± 37	5	NS
pEGFP-N1-vector	mLRP1-Myc (Cy3)	2138 ± 101	5	NS
Myc-LC (11H4-FITC)	None	2305 ± 69	15	—
Myc-LC (11H4-FITC)	BACE-V5 (Cy3)	2100 ± 148	15	$p < 0.0001$
LRP165-Myc (11H4-FITC)	None	2316 ± 86	13	—
LRP165-Myc (11H4-FITC)	BACE-V5 (Cy3)	1803 ± 283	16	$p < 0.0001$

[a] —, signifies control condition.
[b] Not significant.

was measured by hydrolysis of *o*-nitrophenyl-β-D-galactopyranoside in cells lysed with reporter lysis buffer (Promega). Pharmacologic inhibition of LRP cleavage was assessed after overnight treatment with vehicle (Me_2SO) or a cell-permeable, peptidomimetic inhibitor of BACE (Calbiochem) (39).

Western Blotting—N2a cells co-transfected with LC-Myc and either empty vector, BACE, or a catalytically inactive BACE mutant and treated with 1 μM γ-secretase inhibitor DAPT (40) for 12 h (a generous gift from M. Wolfe, Brigham and Women's Hospital, Boston, MA) were lysed in 1% Triton X-100 in TBS buffer and proteinase inhibitor tablets (Roche Applied Science) and then loaded onto 4–20% Tris-glycine polyacrylamide gels (Novex) under denaturing and reducing conditions. The proteins were transferred to polyvinylidene difluoride membrane and LRP light chain was detected by rabbit anti-Myc Ab with Alexa 680 (Molecular Probes) goat anti-rabbit secondary and visualized on a Licor Odyssey near-infrared gel reader (Lincoln, Nebraska).

Luciferase Assay—HEK293 cells were transfected with LRP-Gal4-VP16 (LRP-GV) in the absence or presence of BACE and relative luciferase activity determined (28). Activity relative to β-galactosidase is shown and averaged for triplicate transfection. In all cases transfection was confirmed by immunoblotting.

RESULTS

Localization of BACE and LRP Constructs—We first tested the localization of BACE and LRP in co-expressing H4 cells. When expressed individually, both mLRP1 and BACE were localized mainly in punctate structures in the cells. mLRP1-positive structures largely overlapped with BACE-positive structures when they were co-expressed. To determine the subcellular distribution we immunostained co-expressing H4 cells with organelle markers or, in cell surface stained without Triton X-100 treatment, Alexa555-labeled CTx-B as a raft marker. mLRP1 and BACE co-localized in the endosomal compartments stained by EEA1 (Fig. 2*A*). To a lesser extent, the Golgi marker GM130 also overlapped with mLRP1 and BACE (Fig. 2*B*). On the cell surface Myc-LC and BACE are partly co-localized with one another in lipid rafts. The results of the immunocytochemistry suggest that LC and BACE are co-localized in distinct compartments of the cell including lipid rafts (Fig. 2*C*), Golgi and prominently in the endosomal compartment.

To confirm that LRP localizes to lipid rafts we prepared total membrane and separated CM and NCM fractions using an optiprep gradient. LRP was present in caveolae as well as in noncaveolae fractions (Fig. 2*D*), which is in accordance with our confocal data showing partial overlap with the lipid raft marker CTx-B. We then looked for co-localization under physiological conditions. By staining human brain sections, including the hippocampal formation, we were able to observe similar results in neurons expressing endogenous levels of LRP and BACE (Fig. 3*D*).

Co-immunoprecipitation of BACE and LRP in Human Brain Tissue—From the immunohistochemical experiments that showed robust co-localization in both transfected cells and human brain tissue (Fig. 3*D*), we hypothesized that there may be a close interaction between LRP and BACE. To test whether LRP interacts with BACE, we immunoprecipitated BACE from co-transfected H4 cells and probed for mLRP1 (*lane 1*), controlling for nonspecific interactions by assessing lysates incubated without the pull-down antibody (*lane 2*) or pure lysis buffer (*lane 4*). Immunoreactive bands of ~100 kDa (resembling mature furin-cleaved mLRP1-Myc) and ~140 kDa (resembling unprocessed Golgi and ER forms of mLRP1-Myc) (29) were detected in the immunoprecipitated sample and the whole cell lysate (Fig. 3*A*, *lane 4*). To confirm this interaction, the complementary pull-down experiment was performed. mLRP1 immunoprecipitates were probed by an anti-BACE Ab with the same controls. The doublet bands of ~60 and 75 kDa were detected only in *lane 1* and in the control lysate lane (Fig. 3*B*), suggesting that BACE is present in the mLRP1 immunoprecipitates. The 60-kDa band represents endogenous BACE, whereas the 75-kDa band represents transfected BACE containing a V5-His tag.

To demonstrate a direct interaction of LRP and BACE under physiological conditions in brain, where BACE function is presumed to be important in the pathogenesis of Alzheimer disease, we immunoprecipitated BACE from human brain tissue and probed with an antibody to the LRP light chain. A strong immunoreactive band of ~85 kDa (the expected size of the mature endogenous light chain of LRP, *i.e.* furin-cleaved form) (29) was detected in the sample lane (Fig. 3*C*, *lane 1*). Control precipitate from samples lacking anti-BACE Ab (*lane 2*) showed only a weak immunoreactive band, and samples lacking cell extract (*lane 3*) did not contain this band. Thus, endogenous LRP and BACE co-immunoprecipitate.

Interaction of LRP and BACE by FLIM Analysis—We next used an alternative technique to probe protein-protein proximity to test the idea that the LRP-BACE interaction detected by co-immunoprecipitation occurs in specific cell compartments, and to further evaluate the biochemical parameters of this interaction. We utilized FLIM, a morphology-based FRET tech-

nique that can reveal close protein-protein proximity in intact cells. Fluorescence lifetime is influenced by the surrounding microenvironment and is shortened in the immediate vicinity of a FRET acceptor molecule. The degree of lifetime shortening can be displayed with very high spatial resolution in a pseudocolor-coded image. As shown in Fig. 2, double immunostaining showed subcellular compartment co-localization of BACE and LRP predominantly in endosomal compartments, but this does not necessarily imply a close interaction. We measured changes in the lifetime of the donor fluorophore (either FITC, Alexa 488, or GFP) under different experimental conditions. In the absence of an acceptor fluorophore, the lifetime of FITC conjugated to IgG (hereafter referred to simply as FITC) is ~2300 ps, GFP ~2200 ps, and Alexa 488 is ~1900 ps. If an acceptor fluorophore is present but remains too distant from the donor (*i.e.* there is no interaction), donor lifetimes remain in this range. The lifetime of FITC attached to the C terminus of BACE-V5 alone (2334 ± 72 ps) was significantly shortened when co-expressed mLRP1-Myc was C-terminally labeled by Cy3 (2153 ± 55 ps, $p < 0.0001$), indicating FRET between the two fluorophores (Table I). Equivalent results were obtained when BACE was tagged with GFP and when the acceptor and donor fluorophores were exchanged (Table I). In order to test the idea that the decrease in lifetime observed in the mLRP1-GFP/BACE-V5 FLIM assay was because of FRET, we performed an additional control. mLRP1-GFP and Myc-BACE co-transfected cells were stained with anti-Myc Ab, then labeled with Cy3. In this experiment, the Myc tag was at the N terminus of BACE, across the membrane and, therefore, too distant from the C-terminal GFP on mLRP1-GFP to be detected by FRET. Although there was striking co-localization, no lifetime change was observed. This experiment demonstrates the specificity of the proximity assay in this FLIM-based method of measuring FRET.

FLIM allows analysis of FRET localization by recording the distribution of donor lifetimes on a pixel-by-pixel basis. FITC bound to BACE-V5 in the absence of acceptor has a uniform lifetime and a single lifetime peak (Fig. 4*A*); in the presence of mLRP1-Cy3 acceptor, FITC has two distinct lifetimes and is faster, representing "FRETting" molecules (Fig. 4*B*). Examination of the FLIM images of transfected cells suggests that LRP and BACE interact (red pseudocolor) at the cell surface and in endosomal compartments. Because LRP and BACE co-localize in lipid rafts at the cell surface, we suggest that the interaction detected by FLIM also is lipid raft-associated.

Indeed, additional experiments in which only cell surface Myc-LC (N-terminal Myc) and BACE-NT are immunostained demonstrate FRET (Table II) between BACE and LRP specifically in punctuate structures at the cell surface (Fig. 5*B*). To test the hypothesis that this interaction occurs in rafts we cholesterol depleted the cells and repeated the cell surface FLIM experiment. Cholesterol depletion weakened the interaction of BACE and LRP at the cell surface (Fig. 5*C*). This result strongly suggests that BACE and LRP interact on the cell surface distinctively in lipid rafts.

To further confirm the physiologic interaction of LRP and BACE we performed FLIM in untransfected N2a cells as well as primary cortical neurons, which have relatively abundant BACE and LRP; Alexa 488 was chosen as donor fluorophore because it is somewhat brighter than FITC under the conditions utilized. Statistically shorter lifetimes of the donor in N2a cells (Alexa 488) attached to the C terminus of BACE in the presence of C-terminally Cy3-labeled LRP (1492 ± 293 ps, $p < 0.0001$) compared with only Alexa 488-labeled BACE (1868 ± 116 ps) as well as in FITC-labeled primary neurons attached to the C terminus of BACE in the presence of C-terminally Cy3-labeled LRP (2055 ± 103 ps, $p \leq 0.005$) compared with only FITC-labeled BACE (2193 ± 105 ps) indicate FRET between endogenously expressed proteins (Table III). In the absence of acceptor, Alexa 488 has a uniform lifetime; in the presence of acceptor a second peak appears, reflecting an interaction (Fig. 4, *C–F*). The interaction, pseudocolored red, also appears to be stronger in the distal compartments at or near the cell surface. This result demonstrates close protein-protein interaction between endogenous LRP and endogenous BACE at the cell surface in a neuronal cell type, paralleling the co-immunoprecipitation results.

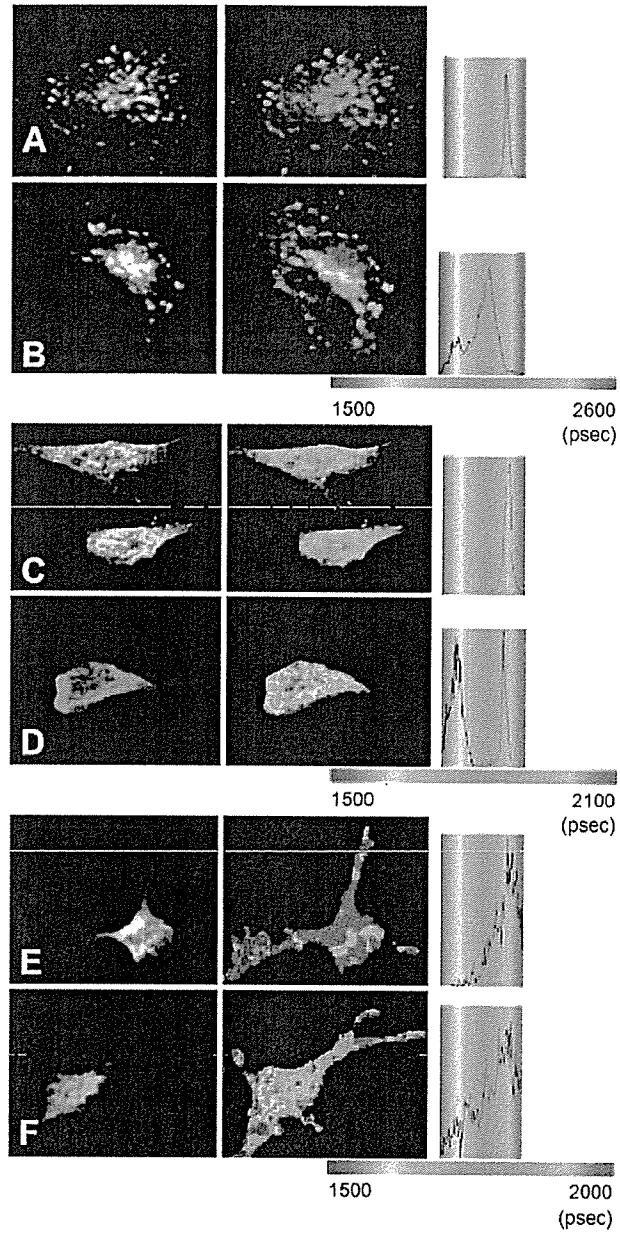

FIG. 4. **FLIM analysis of the proximity between LRP and BACE within cells.** H4 cells were co-transfected with mLRP1-Myc (*A*, unlabeled; *B*, labeled by Cy3) and BACE-V5 (labeled by FITC). N2a cells were stained for endogenous LRP with 11H4 (labeled by Cy3) and anti-BACE CT Ab (labeled by Alexa 488) for the analysis (*D*) or only with the donor fluorophore in the negative control (*C*). Primary neurons were stained for endogenous LRP with 11H4 (Cy3) and Anti-BACE CT Ab (FITC) for the analysis (*F*) or only with the donor fluorophore (*E*). The intensity of the images shows the standard immunostaining pattern for BACE. The color-coded FLIM image shows the lifetimes (ps) of FITC in the presence or absence of donor Cy3.

TABLE II
FLIM assay data

FLIM assay data showing the proximity of LC and BACE and strong weakening of this proximity by cholesterol depletion (Chol. depl.) and substitution of the LRP intracellular domain by LDLR in cell surface staining. H4 cells were co-transfected with Myc-(N terminus)-LC or an LRP-LDLR chimera (labeled by FITC) and BACE-V5 (labeled by Cy3). Cholesterol depletion was performed with lovastatin/mevalonate for 24 h and MβCD for 10 min.

Donor	Acceptor	Chol. depl.[a]	Lifetime	*n*	Significance	
			ps mean ± S.D.			
Myc-LC (FITC)	None	−	2317 ± 109	21	—[d]	—[d]
Myc-LC (FITC)	BACE-NT (Cy3)	−	2023 ± 173	23	$p < 0.0001$[b]	$p < 0.0001$[c]
Myc-LC (FITC)	BACE-NT (Cy3)	+	2203 ± 83	21	$p < 0.001$[b]	—[d]
Myc-LC-LDLR	None	−	2335 ± 111	8	—[d]	$p < 0.005$[c]
Myc-LC-LDLR	BACE-NT (Cy3)	−	2243 ± 143	8	NS[e]	—[d]

[a] Presence (+) or absence (−) of cholesterol depletion.
[b] Significance as compared with control.
[c] Significance as compared with cholesterol depletion.
[d] Signifies control condition.
[e] Not significant.

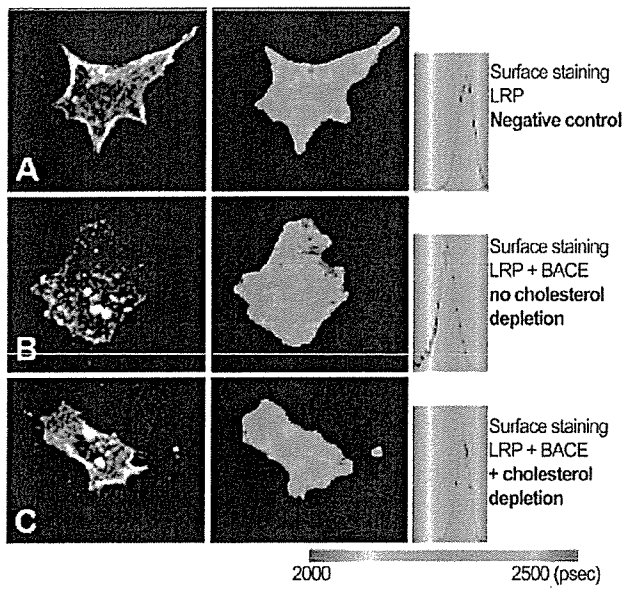

FIG. 5. **FLIM analysis of LC and BACE proximity on cell surface.** H4 cells were co-transfected with Myc-LC (labeled by FITC) and BACE-V5 (*A*, unlabeled; *B* and *C*, labeled by Cy3). Cholesterol depletion was performed with lovastatin/mevalonate for 24 h and MβCD for 10 min (*C*). The intensity image shows a typical immunostaining pattern for surface LRP. The color-coded FLIM image shows the lifetimes (ps) of FITC in the absence (*A*) or presence of the acceptor Cy3 (*B* and *C*). The shorter FITC lifetimes, represented by red-yellow pseudocolor, appear in distinct spots on the cell surface (*B*), and can be abolished by cholesterol depletion (*C*).

To identify the domain of LRP interacting with BACE, we utilized LRP deletion constructs. LC, which contains the β-chain of LRP, and LRP165, a construct that contains only the 100 amino acid intracellular domain, the transmembrane domain and a very small extension beyond the membrane, both interacted strongly with BACE (Table I). This result implicates the intracellular or the transmembrane domain of LRP as the site of interaction. To further test this hypothesis, we utilized a chimeric protein in which the extracellular and transmembrane domains of LC are fused to the intracellular domain of the low density lipoprotein receptor (LDLR) (Fig. 1) and performed FLIM on the cell surface as described above. This construct did not FRET with BACE (Table II), further supporting the importance of the intracellular domain of LRP for this interaction.

There are several scaffold/adaptor proteins known to interact with LRP including Fe65 (22, 23, 41) and mammalian disabled 1 (mDab1) (23). If the intracellular domain is responsible for the interaction between LRP and BACE, these adaptor proteins may play a role in the interaction. We have demonstrated previously that LRP and Fe65 interact using a FRET based cell assay (22), and that Fe65 is responsible for mediating an LRP-Fe65-APP heterotrimeric complex. We therefore examined the possibility that these molecules may interact with BACE by the FRET assay. However, under the conditions utilized we did not detect any FRET between BACE and Fe65 or between BACE and mDab1 (data not shown). Recent data also suggest that phosphorylation of BACE at Ser^{498} changes its trafficking possibly by altering its interactions with GGA by its C-terminal dileucine motif (30, 42). We generated the S498D, S498A, and L499A/L500A mutants of BACE to evaluate if these mutants, which mimic or block phosphorylation of Ser^{498} (15), alter interaction with LRP. No changes in FRET measures were observed with these manipulations (data not shown).

BACE Internalization Assay—Because we observed LRP-BACE interactions dependent on a domain of LRP that mediates APP endocytosis, we hypothesized that LRP might also influence BACE endocytosis and thereby regulate APP cleavage. In order to assess the effect of LRP on BACE endocytosis we assessed internalization of BACE after biotinylation of its N-terminal Myc tag at the cell surface and assayed internalized *versus* cell surface BACE over time (Fig. 6). Co-transfection with LC did not enhance BACE internalization from the cell surface in LRP-null CHO cells (13–5-1) in contrast to known enhancement of APP endocytosis with LC (20). The same results were obtained using PEA13 (LRP−/−) fibroblasts (data not shown). Thus it appears that BACE internalization is not mediated by LRP under these conditions.

LRP Shedding—Because LRP is a known γ-substrate, we hypothesized that it might also be cleaved by β-secretase. In order to assess the effect of BACE and LRP interaction on LRP processing, we measured shedding of the extracellular domain of LRP with the cDNA of SEAP fused to the N terminus of the LRP β-chain. An analogous construct has been used to study BACE cleavage of APP (43). After co-transfection of the SEAP-LRP construct with a β-galactosidase reporter construct and either empty vector, WT-BACE or BACE D93/289A, SEAP activity was measured in the medium and normalized to β-galactosidase activity. WT-BACE led to a significant increase in LRP ectodomain shedding compared with baseline, whereas, as expected, catalytically inactive BACE D93/289A exhibited no effect (Fig. 7*A*). To confirm that LRP is cleaved by BACE, we used two additional approaches. Overnight treatment with a cell-permeable BACE inhibitor (39) reduced LRP cleavage

TABLE III
FLIM assay data showing the proximity of endogenous LRP and BACE in N2a cells and in primary neurons.

	Donor	Acceptor	Lifetime	*n*	Significance (compared to control)
			ps mean ± S.D.		
N2a cells	BACE-CT (Alexa 488)	None	1868 ± 116	20	—[a]
	BACE-CT (Alexa 488)	11H4 (Cy3)	1492 ± 293	20	$p < 0.0001$
Primary neurons	BACE-CT (FITC)	None	2193 ± 105	15	—[a]
	BACE-CT (FITC)	11H4 (Cy3)	2055 ± 108	10	$p \leq 0.005$

[a] — Signifies control condition.

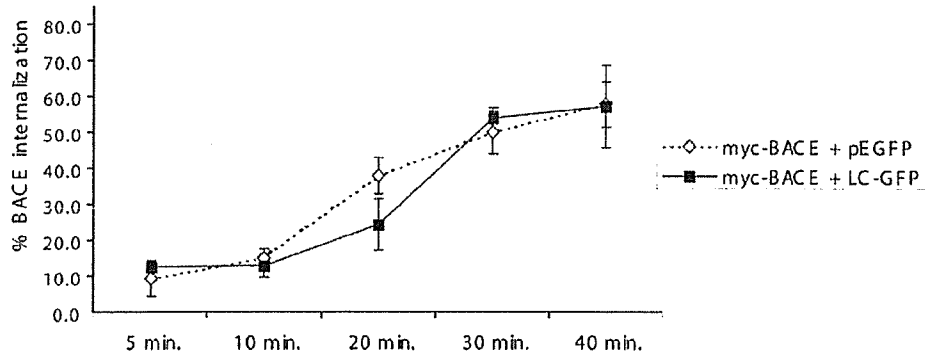

FIG. 6. **BACE internalization assay.** Internalization of biotinylated Myc-BACE was monitored over 40 min in LRP-null CHO (13-5-1) cells co-transfected with either empty vector (pEGFP ◇) or LC-GFP (♦). No change of the basic endocytosis rate of BACE with LRP co-transfection was observed. Given are the means and S.D. of one of three independent assays. Both transfection and measurement were carried out in triplicate.

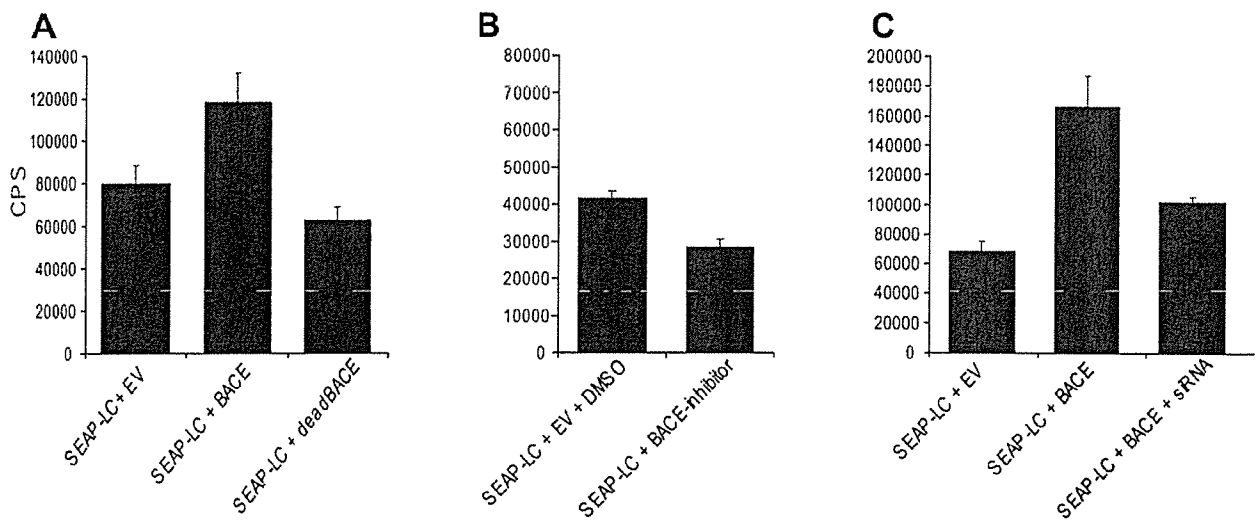

FIG. 7. **LRP shedding assay.** *A*, HEK cells were transfected with SEAP-LRP, β-galactosidase, and empty vector or with a plasmid encoding WT-BACE or a catalytically inactive BACE mutant (BACE D93/289A). *B*, HEK cells were transfected with SEAP-LRP, β-galactosidase, and empty vector and treated overnight with either Me_2SO (*DMSO*) or 12.5 μM BACE-inhibitor II. *C*, HEK cells were transfected with SEAP-LRP, β-galactosidase, and WT-BACE, and BACE-siRNA. Shown is the alkaline phosphatase activity in the conditioned medium normalized to β-galactosidase activity. Given are the means and S.D. of one of three independent assays. Both transfection and measurement were carried out in duplicate or triplicate.

when treating cells that expressed BACE at endogenous levels, indicating that the observed effect has physiologic relevance and is not restricted to cells overexpressing BACE (Fig. 7*B*). The second approach to inactivating BACE utilized siRNA-mediated silencing. Knocking down overexpressed BACE by co-transfection of BACE1-specific siRNA reduced processing of LRP by BACE (Fig. 7*C*).

LRP C-terminal Fragment (CTF) Production after BACE Co-transfection—After treatment with DAPT for 12 h we observed an increase of the LRP-CTF 25-kDa band consistent with the observations of (28) suggesting γ-cleavage of LRP. We hypothesized that, like APP, the direct substrate of γ-secretase activity would be an N-terminally cleaved form of LRP. To determine if BACE activity would produce an LRP-derived γ-secretase substrate, we co-transfected LC with BACE. This led to an increase of LRP-CTF detected by Western blot as a 25-kDa band. To confirm that this band is the substrate of γ-secretase activity, we repeated this experiment in the presence of the γ-secretase inhibitor DAPT, and detected an increased amount of the 25-kDa product. The presence of BACE further increased and co-transfection with catalytically inactive BACE mutant did not increase this band intensity (Fig. 8). These results are consistent with a BACE-mediated cleavage of LRP, generating a CTF for γ-cleavage.

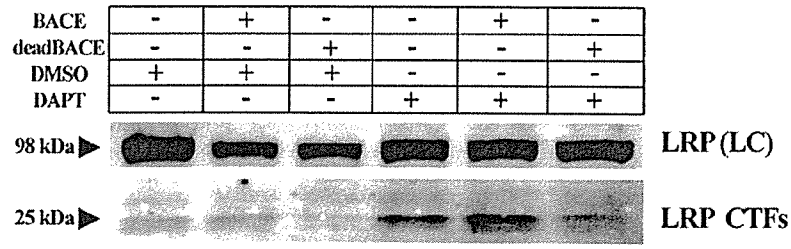

FIG. 8. **LRP CTF Western blot.** N2a cells co-transfected with LC-Myc and either empty vector, BACE, or a catalytically inactive BACE mutant (*deadBACE*) were treated with vehicle (*DMSO*) or DAPT (12 h). Increases of CTF intensity were detected after DAPT treatment and/or BACE co-transfection. Shown is the intensity of a representative blot out of four experiments without DAPT treatment and two with DAPT treatment.

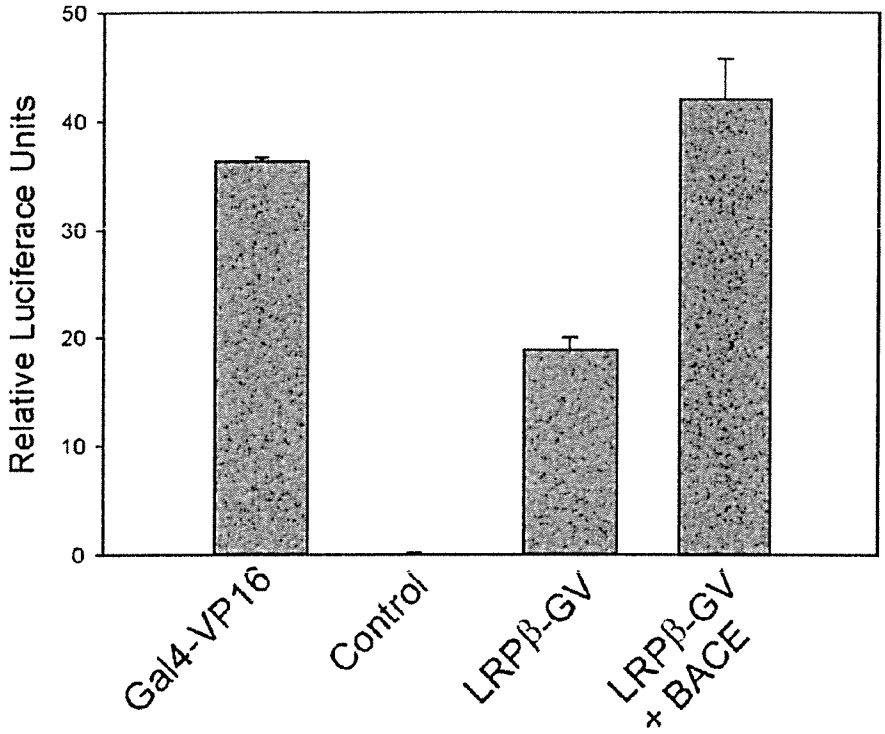

FIG. 9. **BACE increases release of LRP-ICD.** HEK293 cells were transfected with LRP-Gal4/VP16 (28) in the absence or presence of BACE, and luciferase activity determined. Activity relative to β-galactosidase is shown as the average of triplicate analyses. The addition of BACE led to a statistically significant increase in luciferase activity, suggesting that LRP undergoes BACE cleavage, and leading to subsequent release of the cytoplasmic domain and translocation to the nucleus to activate the Gal4 assay.

Luciferase Assay—LRP interaction with β-secretase leads to LRP cleavage and generation of a truncated form. By analogy to APP, it may then undergo further proteolysis and release the LRP-ICD fragment. Evidence that LRP is itself a γ-substrate has been presented using an LRP-Gal4/VP16 construct utilizing a luciferase reporter assay for LRP C-terminal cleavage (28). We used this same assay to determine if co-transfection with BACE would alter generation of this putative signaling domain. Co-transfection with BACE led to a substantial increase in luciferase activity suggesting that LRP undergoes BACE cleavage, leading ultimately to release of the cytoplasmic domain and translocation to the nucleus (Fig. 9).

DISCUSSION

In the present study, we have demonstrated that BACE interacts with the intracellular domain of LRP, a multifunctional endocytic receptor. The interaction was demonstrated by co-immunoprecipitation of BACE and LRP from overexpressing cells and from endogenous BACE and LRP in human brain samples and primary neurons. Co-localization and close proximity in both H4 and N2a cells was shown by confocal microscopy and FRET-based proximity assays, suggesting co-localization primarily in endosomes and at the cell surface. Cholesterol depletion disrupted the cell surface LRP interaction, suggesting that the interaction occurs in lipid rafts.

The FRET technique used here, FLIM, is advantageous because it provides quantitative data on protein-protein proximity with exquisite subcellular localization. The two fluorophores must be quite close (<10 nm) to support FRET; tagging LRP and BACE molecules "across the membrane" from one another or after cholesterol depletion abolishes FRET despite continued co-localization at the light level. Analogous results were obtained using three different fluorophores, multiple different antibody pairs, endogenous or transfected LRP and BACE, and two different cell types. Taken together with the co-immunoprecipitation data, our results strongly support the conclusion that LRP and BACE interact at the cell surface in raft compartments.

In contrast to γ-secretase, where at least 15 substrates have been described (44), BACE has so far appeared to be relatively specific. Sialyltransferase and PSGL-1, in addition to APP and its homologues APLP1 and 2 are the only other reported substrates of BACE (6, 43). A family of GGA adaptor proteins and the phospholipid scramblase 1 (PLSCR1) have been shown to directly interact with the BACE tail (42, 45). Interestingly, both BACE and PLSCR1 were localized in a low buoyant lipid microdomain, a potential site of interaction with APP and LRP.

In summary, our data demonstrate a close interaction of LRP and BACE in specific subcellular compartments. Although BACE and LRP are mostly co-localized in the endosomal compartments and to a lesser extent in the Golgi and on the cell surface as shown by conventional immunostaining, our FLIM data suggest that they come into closest proximity at the cell surface in lipid rafts, where it has been shown that amyloidogenic processing seems to occur in raft associated compart-

ments (13). This is in good accordance with a recent article showing that ApoE, a LRP ligand, is co-localized with APP and BACE in lipid rafts (46). Moreover, our SEAP-LC assay demonstrates that BACE-mediated cleavage of the LRP extracellular domain leads to secretion of the shed domain into the extracellular milieu. Because even the LRP165 construct (which lacks ligand binding domains and most of the extracellular part of LRP) interacts with the BACE intracellular domain and the LC-LDLR-chimera lacking the LRP intracellular domain did not interact with BACE, we postulate that the major interaction site is the intracellular domain of LRP. Whereas two candidate adaptor proteins, Fe65 and mDab, did not appear to mediate the interaction, multiple other potential adaptor proteins might either mediate or impact this interaction. Surprisingly we did not find enhancement of BACE endocytosis in LRP-null cells co-transfected with LRP. Thus, although LRP co-traffics with BACE to the cell surface, it does not appear to be critical for BACE recycling from the cell surface to endosomes. Our current data, showing an interaction between LRP and BACE, when viewed in the context of previous studies of APP-LRP interactions, suggest that LRP has a complex role in modulating APP processing. The LRP C-terminal domain also mediates an interaction with APP in similar cell compartments (22). Thus, LRP, which is highly enriched in rafts, potentially acts as a scaffolding complex in rafts for APP and for BACE; such an interaction may help explain the observations that directing APP to rafts enhances β-cleavage and Aβ generation (13).

We found that BACE activity at endogenous levels leads to an increase of secreted LRP in the medium as well as LRP-CTF, analogous to APP processing. Thus we now show that LRP is a substrate for both BACE and γ-secretase, identified as APP-processing enzymes. Whether this processing leads to a stable LRP equivalent of Aβ is unknown. Moreover BACE overexpression leads to an increase of γ-secretase-like cleavage to release LRP-ICD. Although LRP-ICD has been shown to translocate to the nucleus and interact with Fe65 and Tip60 (28, 47), whether or not it has a transcriptional role under physiological conditions remains unknown. However, both LRP (48, 49) and other members of the LDL receptor-related family (50) have been implicated as having signaling roles in neurons, and it seems likely that the cleavage of LRP we observe could modulate such signaling. Further studies will be needed to elucidate if APP and LRP act co-operatively or competitively for access to these secretases and how interactions of LRP with other ligands impact these processes.

Acknowledgments—We thank Hibiki Kawamata and Tejal Shah for assisting in the initial portion of this work. We thank the Massachusetts Alzheimer Disease Research Center Brain bank for brain samples.

REFERENCES

1. Vassar, R., Bennett, B. D., Babu-Khan, S., Kahn, S., Mendiaz, E. A., Denis, P., Teplow, D. B., Ross, S., Amarante, P., Loeloff, R., Luo, Y., Fisher, S., Fuller, J., Edenson, S., Lile, J., Jarosinski, M. A., Biere, A. L., Curran, E., Burgess, T., Louis, J. C., Collins, F., Treanor, J., Rogers, G., and Citron, M. (1999) *Science* **286,** 735–741
2. Sinha, S., Anderson, J. P., Barbour, R., Basi, G. S., Caccavello, R., Davis, D., Doan, M., Dovey, H. F., Frigon, N., Hong, J., Jacobson-Croak, K., Jewett, N., Keim, P., Knops, J., Lieberburg, I., Power, M., Tan, H., Tatsuno, G., Tung, J., Schenk, D., Seubert, P., Suomensaari, S. M., Wang, S., Walker, D., Zhao, J., McConlogue, L., and John, V. (1999) *Nature* **402,** 537–540
3. Yan, R., Bienkowski, M. J., Shuck, M. E., Miao, H., Tory, M. C., Pauley, A. M., Brashier, J. R., Stratman, N. C., Mathews, W. R., Buhl, A. E., Carter, D. B., Tomasselli, A. G., Parodi, L. A., Heinrikson, R. L., and Gurney, M. E. (1999) *Nature* **402,** 533–537
4. Hussain, I., Powell, D., Howlett, D. R., Tew, D. G., Meek, T. D., Chapman, C., Gloger, I. S., Murphy, K. E., Southan, C. D., Ryan, D. M., Smith, T. S., Simmons, D. L., Walsh, F. S., Dingwall, C., and Christie, G. (1999) *Mol. Cell Neurosci.* **14,** 419–427
5. Li, Q., and Sudhof, T. C. (2004) *J. Biol. Chem.* **279,** 10542–10550
6. Kitazume, S., Tachida, Y., Oka, R., Shirotani, K., Saido, T. C., and Hashimoto, Y. (2001) *Proc. Natl. Acad. Sci. U. S. A.* **98,** 13554–13559
7. Bennett, B. D., Denis, P., Haniu, M., Teplow, D. B., Kahn, S., Louis, J. C., Citron, M., and Vassar, R. (2000) *J. Biol. Chem.* **275,** 37712–37717
8. Capell, A., Steiner, H., Willem, M., Kaiser, H., Meyer, C., Walter, J., Lammich, S., Multhaup, G., and Haass, C. (2000) *J. Biol. Chem.* **275,** 30849–30854
9. Creemers, J. W., Ines Dominguez, D., Plets, E., Serneels, L., Taylor, N. A., Multhaup, G., Craessaerts, K., Annaert, W., and De Strooper, B. (2001) *J. Biol. Chem.* **276,** 4211–4217
10. Kinoshita, A., Fukumoto, H., Shah, T., Whelan, C. M., Irizarry, M. C., and Hyman, B. T. (2003) *J. Cell Sci.* **116,** 3339–3346
11. Huse, J. T., Pijak, D. S., Leslie, G. J., Lee, V. M., and Doms, R. W. (2000) *J. Biol. Chem.* **275,** 33729–33737
12. Riddell, D. R., Christie, G., Hussain, I., and Dingwall, C. (2001) *Curr. Biol.* **11,** 1288–1293
13. Ehehalt, R., Keller, P., Haass, C., Thiele, C., and Simons, K. (2003) *J. Cell Biol.* **160,** 113–123
14. Cordy, J. M., Hussain, I., Dingwall, C., Hooper, N. M., and Turner, A. J. (2003) *Proc. Natl. Acad. Sci. U. S. A.* **100,** 11735–11740
15. Walter, J., Fluhrer, R., Hartung, B., Willem, M., Kaether, C., Capell, A., Lammich, S., Multhaup, G., and Haass, C. (2001) *J. Biol. Chem.* **276,** 14634–14641
16. Herz, J., and Strickland, D. K. (2001) *J. Clin. Investig.* **108,** 779–784
17. Li, Y., Cam, J., and Bu, G. (2001) *Mol. Neurobiol.* **23,** 53–67
18. Kounnas, M. Z., Moir, R. D., Rebeck, G. W., Bush, A. I., Argraves, W. S., Tanzi, R. E., Hyman, B. T., and Strickland, D. K. (1995) *Cell* **82,** 331–340
19. Ulery, P. G., Beers, J., Mikhailenko, I., Tanzi, R. E., Rebeck, G. W., Hyman, B. T., and Strickland, D. K. (2000) *J. Biol. Chem.* **275,** 7410–7415
20. Pietrzik, C. U., Busse, T., Merriam, D. E., Weggen, S., and Koo, E. H. (2002) *EMBO J.* **21,** 5691–5700
21. Rebeck, G. W., Moir, R. D., Mui, S., Strickland, D. K., Tanzi, R. E., and Hyman, B. T. (2001) *Brain Res. Mol. Brain Res.* **87,** 238–245
22. Kinoshita, A., Whelan, C. M., Smith, C. J., Mikhailenko, I., Rebeck, G. W., Strickland, D. K., and Hyman, B. T. (2001) *J. Neurosci.* **21,** 8354–8361
23. Trommsdorff, M., Borg, J. P., Margolis, B., and Herz, J. (1998) *J. Biol. Chem.* **273,** 33556–33560
24. Quinn, K. A., Pye, V. J., Dai, Y. P., Chesterman, C. N., and Owensby, D. A. (1999) *Exp. Cell Res.* **251,** 433–441
25. Rozanov, D. V., Hahn-Dantona, E., Strickland, D. K., and Strongin, A. Y. (2004) *J. Biol. Chem.* **279,** 4260–4268
26. Higashi, S., and Miyazaki, K. (2003) *Biochemistry* **42,** 6514–6526
27. Kinoshita, A., Shah, T., Tangredi, M. M., Strickland, D. K., and Hyman, B. T. (2003) *J. Biol. Chem.* **278,** 41182–41188
28. May, P., Reddy, Y. K., and Herz, J. (2002) *J. Biol. Chem.* **277,** 18736–18743
29. Mikhailenko, I., Battey, F. D., Migliorini, M., Ruiz, J. F., Argraves, K., Moayeri, M., and Strickland, D. K. (2001) *J. Biol. Chem.* **276,** 39484–39491
30. von Arnim, C. A., Tangredi, M. M., Peltan, I. D., Lee, B. M., Irizarry, M. C., Kinoshita, A., and Hyman, B. T. (2004) *J. Cell Sci.* **117,** 5437–5445
31. Kao, S.-C., Krichevsky, A. M., Kosik, K. S., and Tsai, L.-H. (2004) *J. Biol. Chem.* **279,** 1942–1949
32. Berezovska, O., Frosch, M., McLean, P., Knowles, R., Koo, E., Kang, D., Shen, J., Lu, F. M., Lux, S. E., Tonegawa, S., and Hyman, B. T. (1999) *Brain Res. Mol. Brain Res.* **69,** 273–280
33. Smart, E. J., Ying, Y. S., Mineo, C., and Anderson, R. G. (1995) *Proc. Natl. Acad. Sci. U. S. A.* **92,** 10104–10108
34. Liscum, L., Arnio, E., Anthony, M., Howley, A., Sturley, S. L., and Agler, M. (2002) *J. Lipid Res.* **43,** 1708–1717
35. Orlando, L. R., Dunah, A. W., Standaert, D. G., and Young, A. B. (2002) *Neuropharmacology* **43,** 161–173
36. Berezovska, O., Ramdya, P., Skoch, J., Wolfe, M. S., Bacskai, B. J., and Hyman, B. T. (2003) *J. Neurosci.* **23,** 4560–4566
37. Bacskai, B. J., Skoch, J., Hickey, G. A., Allen, R., and Hyman, B. T. (2003) *J. Biomed. Opt.* **8,** 368–375
38. Sever, S., Damke, H., and Schmid, S. L. (2000) *J. Cell Biol.* **150,** 1137–1148
39. Abbenante, G., Kovacs, D. M., Leung, D. L., Craik, D. J., Tanzi, R. E., and Fairlie, D. P. (2000) *Biochem. Biophys. Res. Commun.* **268,** 133–135
40. Kornilova, A. Y., Das, C., and Wolfe, M. S. (2003) *J. Biol. Chem.* **278,** 16470–16473
41. Pietrzik, C. U., Yoon, I. S., Jaeger, S., Busse, T., Weggen, S., and Koo, E. H. (2004) *J. Neurosci.* **24,** 4259–4265
42. He, X., Chang, W. P., Koelsch, G., and Tang, J. (2002) *FEBS Lett.* **524,** 183–187
43. Lichtenthaler, S. F., Dominguez, D. I., Westmeyer, G. G., Reiss, K., Haass, C., Saftig, P., De Strooper, B., and Seed, B. (2003) *J. Biol. Chem.* **278,** 48713–48719
44. De Strooper, B. (2003) *Neuron* **38,** 9–12
45. Kametaka, S., Shibata, M., Moroe, K., Kanamori, S., Ohsawa, Y., Waguri, S., Sims, P. J., Emoto, K., Umeda, M., and Uchiyama, Y. (2003) *J. Biol. Chem.* **278,** 15239–15245
46. Kawarabayashi, T., Shoji, M., Younkin, L. H., Wen-Lang, L., Dickson, D. W., Murakami, T., Matsubara, E., Abe, K., Ashe, K. H., and Younkin, S. G. (2004) *J. Neurosci.* **24,** 3801–3809
47. Kinoshita, A., Whelan, C. M., Berezovska, O., and Hyman, B. T. (2002) *J. Biol. Chem.* **277,** 28530–28536
48. Bacskai, B. J., Xia, M. Q., Strickland, D. K., Rebeck, G. W., and Hyman, B. T. (2000) *Proc. Natl. Acad. Sci. U. S. A.* **97,** 11551–11556
49. Boucher, P., Liu, P., Gotthardt, M., Hiesberger, T., Anderson, R. G., and Herz, J. (2002) *J. Biol. Chem.* **277,** 15507–15513
50. Trommsdorff, M., Gotthardt, M., Hiesberger, T., Shelton, J., Stockinger, W., Nimpf, J., Hammer, R. E., Richardson, J. A., and Herz, J. (1999) *Cell* **97,** 689–701